Asymmetric fission for ^{70,76}Se and ^{90,94,98}Mo via quasi-molecular shapes and related formulas

G. Royer, K. Zbiri [1]

Laboratoire Subatech, UMR: IN2P3/CNRS-Université-Ecole des Mines,

4, rue A. Kastler, 44307 Nantes Cedex 03, France

NAME

Asymmetric fission for ^{70,76}Se and ^{90,94,98}Mo via quasi-molecular shapes and related formulas

G. Royer, K. Zbiri [1]

Laboratoire Subatech, UMR: IN2P3/CNRS-Université-Ecole des Mines, 4 rue A. Kastler, 44307 Nantes Cedex 03, France

Abstract

The asymmetric fission has been described within quasi-molecular shapes and a Generalized Liquid Drop Model including the nuclear proximity energy. The fission barrier heights agree with the recent data obtained for ^{70,76}Se and ^{90,94,98}Mo. An analytical formula given the temperature-dependent fission barrier height as functions of the charges and masses of the parent nucleus and of one fragment is proposed. Another expression allows to obtain for a fixed fragment charge the associated most probable mass.

PACS: 24.75.+i; 25.70.Jj; 21.60.Ev
Keywords: Asymmetric fission; Liquid Drop Model; Proximity energy.

[1] E-mail:royer@subatech.in2p3.fr

1 Introduction

Heavy-ion fusion allows to explore the asymmetric fission of medium and light nuclei. Excitation functions of the emitted intermediate mass fragments are accessible and macroscopic asymmetric fission barrier heights have been extracted [1–4]. For the light nuclei located below the Businaro-Gallone point the fission barrier height decreases monotonically with the decay asymmetry and the light-particle emission is the main exit channel. Nevertheless, very recently, the excitation functions for fragments with Z=5-25 emitted from the isotopes ^{90,94,98}Mo produced in the reactions ^{78,82,86}Kr+^{12}C have been obtained as for fragments with Z=5-20 emitted from the isotopes ^{70,76}Se produced in the reactions ^{58,64}Ni+^{12}C [5,6].
These new data allow to compare the ability of the different macroscopic models to describe this rare decay mode intermediate between symmetric fission and light-particle emission. It has been found that the rotating liquid drop model (RLDM) overestimates the shell-corrected macroscopic fission barrier heights by several MeV while the rotating finite-range model (RFRM) [7,8] strongly underestimates the data, the difference between the models differing by as much as 10 MeV.
The purpose of this work is to study to what extent the generalized liquid drop model (GLDM) and a quasi-molecular shape sequence which have allowed to reproduce reasonably well most fusion, fission, α and cluster radioactivity data [9–12] are also able to describe the asymmetric fission data on light nuclei, without any change of the parameters. For global studies and statistical codes, analytical formulas given the temperature-dependent fission barrier height as functions of the charges and masses of the parent nucleus and of one fragment are proposed.

2 Generalized Liquid Drop Model and quasi-molecular shapes

Within the GLDM the macroscopic energy of a deformed nucleus is defined as [10]

$$E = E_V + E_S + E_C + E_N. \tag{1}$$

For one-body shapes, the volume E_V, surface E_S and Coulomb E_C energies are given by:

$$E_V = -15.494(1 - 1.8I^2)A(1 + 0.00337T^2)\ MeV, \tag{2}$$

$$E_S = 17.9439(1 - 2.6I^2)A^{2/3}(S/4\pi R_0^2)(1 + 1.5T/17)(1 - T/17)^{3/2}\ MeV, \tag{3}$$

$$E_C = 0.6e^2(Z^2/R_0) \times 0.5 \int (V(\theta)/V_0)(R(\theta)/R_0)^3 \sin\theta d\theta. \qquad (4)$$

I is the relative neutron excess and S the surface of the deformed nucleus. $V(\theta)$ is the electrostatic potential at the surface and V_0 the surface potential of the sphere.
When the spherical fragments are separated:

$$E_{V12} = -15.494 \left[(1-1.8I_1^2)A_1 + (1-1.8I_2^2)A_2\right](1+0.00337T^2)\ MeV, (5)$$

$$E_{S12} = 17.9439 \left[(1-2.6I_1^2)A_1^{2/3} + (1-2.6I_2^2)A_2^{2/3}\right](1+1.5T/17)(1-T/17)^{3/2}\ MeV, (6)$$

$$E_{C12} = 0.6e^2Z_1^2/R_1 + 0.6e^2Z_2^2/R_2 + e^2Z_1Z_2/r, \qquad (7)$$

where A_i,Z_i,R_i and I_i are the masses, charges, radii and relative neutron excesses of the fragments. r is the distance between the mass centres.
The effective sharp radii $R_{i(i=1,2)}$ have been chosen as:

$$R_i = (1.28A_i^{1/3} - 0.76 + 0.8Ai^{-1/3})(1+0.0007T^2)\ fm. \qquad (8)$$

This later formula often used only to determine the proximity energy allows to take into account the experimentally observed increase of the ratio $r_i = R_i/A_i^{1/3}$ with the mass; for example, $r_0 = 1.10fm$ for ^{14}C and $r_0 = 1.18fm$ for ^{248}Cm. The radius of the compound nucleus has been calculated from the radii of the two fragments assuming volume conservation.
For comparison, in the RLDM and RFRM approaches [7,8], the reduced radius r_0 is respectively $1.225fm$ and $1.16fm$ with any mass dependence while the surface coefficient a_s takes on the values $17.94MeV$ and $21.13MeV$. The GLDM adopts the lowest values of a_s and r_0 (in average) as it is generally accepted now.
The surface energy E_S takes into account the surface tension forces in a half space and does not include the contribution due to the attractive nuclear forces between the surfaces in regard in the neck or the gap between the fragments. The nuclear proximity energy term E_N allows to take into account these additional surface effects when a neck or a gap appears. It has been firstly introduced to describe the fusion process of two close nuclei. It is unfortunately still often neglected in fission studies, which seems valid only for shapes without neck as ellipsoids or for elongated shapes with a very shallow neck. This term is essential to describe smoothly the one-body to two-body transition. For example, at the contact point between two spherical ^{35}Cl fragments the proximity energy reaches $-29MeV$.

$$E_N(r) = 2\gamma \int_{h_{min}}^{h_{max}} \Phi\left[D(r,h)/b\right] 2\pi h dh, \tag{9}$$

where h is the transverse distance varying from the neck radius or zero to the height of the neck border. D is the distance between the opposite surfaces in regard and b the surface width fixed at $0.99(1+0.009T^2)fm$. Φ is the proximity function of Feldmeier [13]. The surface parameter γ is the geometric mean between the surface parameters of the two fragments:

$$\gamma = 0.9517\sqrt{(1-2.6I_1^2)(1-2.6I_2^2)}\ MeVfm^{-2}. \tag{10}$$

In this GLDM the surface diffuseness is not taken into account and the proximity energy vanishes when there is no neck as for ellipsoids for example.
The deformation path previously used to describe the fusion [10], fission [14] and α and cluster emissions [11,12] has been retained since the asymmetric fission connects the symmetric fission and the cluster emission. The shape sequence leads rapidly to the formation of a deep neck while keeping almost spherical ends and to tangent spherical fragments which separate immediately before reaching the top of the potential barrier. Similar compact quasi-molecular shapes have been also assumed to calculate the deformation energy of very heavy nuclei synthesized by fusion reactions [15] and of rotating highly deformed nuclear states [16,17].
The validity of the combination of this GLDM and this shape sequence is warranted by its efficiency to reproduce accurately the fusion barrier heights and radii, the symmetric fission and the α and cluster radioactivity data.

3 Macroscopic fission barrier height for ^{70,76}Se and ^{90,94,98}Mo

The macroscopic fission barrier heights calculated from the GLDM in this quasi-molecular shape path are compared for ^{70,76}Se and ^{90,94,98}Mo with the experimental barrier heights corrected for shell effects and the RLDM and RFRM predictions in figures 1-3. For the compound nuclei ^{70,76}Se the experimental data are on average 13% greater than the RFRM calculations and 21% smaller than those from the RLDM. For ^{90,94,98}Mo the data also fall in between the two model calculations with an important discrepancy. The values given by the GLDM are systematically between the ones of the RLDM and RFRM and in better agreement with the experimental data.
This strongly supports the definition of the GLDM deformation energy and

mainly the selected parameter set which has never been changed as well as the basic idea of a two separated nuclei configuration at the potential barrier top. This last hypothesis is highly realistic when the nuclear proximity energy is properly taken into account. The need to introduce a congruence term [5,6] in the liquid drop model to obtain correct theoretical values of the asymmetric fission barrier heights is not obvious.

4 Analytic formulas for the asymmetric fission barrier height

A set of analytical formulas derived from this GLDM has been previously proposed [18,11,12,19] to calculate rapidly the fusion barrier height and radius, the proximity energy, the partial half-lives for α and cluster decays and some fission characteristics.
The above quantitative agreement has led also to search for and to propose the following analytical formula reproducing accurately the temperature-dependent asymmetric fission barrier heights calculated with the GLDM.

$$E_{bar}(A_1, Z_1, A_2, Z_2, T) = \frac{2.1388 Z_1 Z_2 + 59.427(A_1^{1/3} + A_2^{2/3}) - 27.07 \ln \frac{Z_1 Z_2}{A_1^{1/3} + A_2^{1/3}}}{(A_1^{1/3} + A_2^{1/3})(2.97 - 0.12 \ln Z_1 Z_2)(1 + 0.0015 T^2)} \\ -19.75 + 0.0086(A_1 + A_2) - Q \ MeV \ . \quad (11)$$

where the Q value is simply given by

$$Q = E_V + E_S(sphere) + E_C(sphere) - [E_{V12} + E_{S12} + E_{C12}(\infty)] \ MeV (12)$$

with

$$E_C(sphere) = 0.6 e^2 Z^2 / R_0 \ MeV. \quad (13)$$

For a given charge Z_1 of the heaviest fragment, the mass which corresponds to the lowest asymmetric fission barrier height can be taken as

$$A_1 = \frac{A}{2} + \frac{2Z_1 - Z + \sqrt{Z_1^2 + 40 Z_1 + 10^4} - \sqrt{(Z - Z_1)^2 + 40(Z - Z_1) + 10^4}}{1.2}. (14)$$

In table 1, the predictions of the GLDM for the fission barrier height of light and intermediate mass nuclei are given for different asymmetries. As in the Businaro-Gallone picture the fission barrier height decreases monotically for the light nuclei with the asymmetry while for the heavy nuclei the symmetric fission is stable with respect to the mass-asymmetry mode and the potential

barrier height reaches a maximum for intermediate asymmetry and diminishes for the highest asymmetry corresponding to the light particle emission.
The dependence on the temperature of the fission barrier height is displayed in figures 4 and 5 for two nuclei, one below and one above the Businaro-Gallone point. The heating of a nucleus strongly lowers its fission barrier and the lowering is all the more important as the system is heavy since the essential effect of the temperature is to diminish the surface tension. Nevertheless, the incorporation of temperature maintains essentially the same topology of the Businaro-Gallone picture.

5 Conclusion

The asymmetric fission has been described within a generalized liquid drop model including the nuclear proximity energy and quasi-molecular shapes. Any parameter of this model has been changed since the first studies on fusion, fission, cluster and α emissions. The asymmetric fission barrier heights agree with the recent data obtained for ^{70,76}Se and ^{90,94,98}Mo. This indicates that compact nuclei divide rapidly into spherical fragments and, consequently, that the proximity energy plays a main role in the decay.
An analytical formula given the temperature-dependent fission barrier height as functions of the charges and masses of the parent nucleus and of the fragments is proposed. The corresponding heights in the whole mass and charge range are produced in a table. The most probable mass associated with a fixed fragment charge is given by another expression. A simple fortran code fisfusan.f is available by e-mail.

References

[1] N. Carjan, J.M. Alexander, Phys. Rev. C 38 (1988) 1692.

[2] N. Carjan, M. Kaplan, Phys. Rev. C 45 (1992) 2185.

[3] J. Boger, J.M. Alexander, Phys. Rev. C 50 (1994) 1006.

[4] L.G. Moretto, K.X. Jing, G.J. Wozniak, Phys. Rev. Lett. 74 (1995) 3557.

[5] K.X. Jing, L.G. Moretto, A.C. Veeck, N. Colonna, I. Lhenry, K. Tso, K. Hanold, W. Skulski, Q. Sui, G.J. Wozniak, Nucl. Phys. A 645 (1999) 203.

[6] T.S. Fan, K.X. Jing, L. Phair, K. Tso, M. McMahan, K. Hanold, G.J. Wozniak, L.G. Moretto, Nucl. Phys. A 679 (2000) 121.

[7] A.J. Sierk, Phys. Rev. Lett. 55 (1985) 582.

[8] A.J. Sierk, Phys. Rev. C 33 (1986) 2039.

[9] G. Royer and B. Remaud, J. Phys. G 10 (1984) 1057.

[10] G. Royer and B. Remaud, Nucl. Phys. A 444 (1985) 477.

[11] G. Royer, J. Phys. G 26 (2000) 1149.

[12] G. Royer, R. Moustabchir, Nucl. Phys. A 683 (2001) 182.

[13] H. Feldmeier, 12^{th}Summer School on Nuclear Physics, Mikolajki, Poland, 1979.

[14] G. Royer, in: Heavy Elements and Related New Phenomena, ed. R. K. Gupta and W. Greiner (World Scientific, 1999) p.591.

[15] R. Gherghescu, D.N. Poenaru, W. Greiner, J. Phys. G 23 (1997) 1715.

[16] G. Royer and F. Haddad, Phys. Rev. C 47 (1993) 1302.

[17] T.M. Shneidman, G.G. Adamian, N.V. Antonenko, S.P. Ivanova, W. Scheid, Nucl. Phys. A 671 (2000) 119.

[18] G. Royer, C. Normand, E. Druet, Nucl. Phys. A 634 (1998) 267.

[19] R. Moustabchir, G. Royer, Nucl. Phys. A 683 (2001) 266.

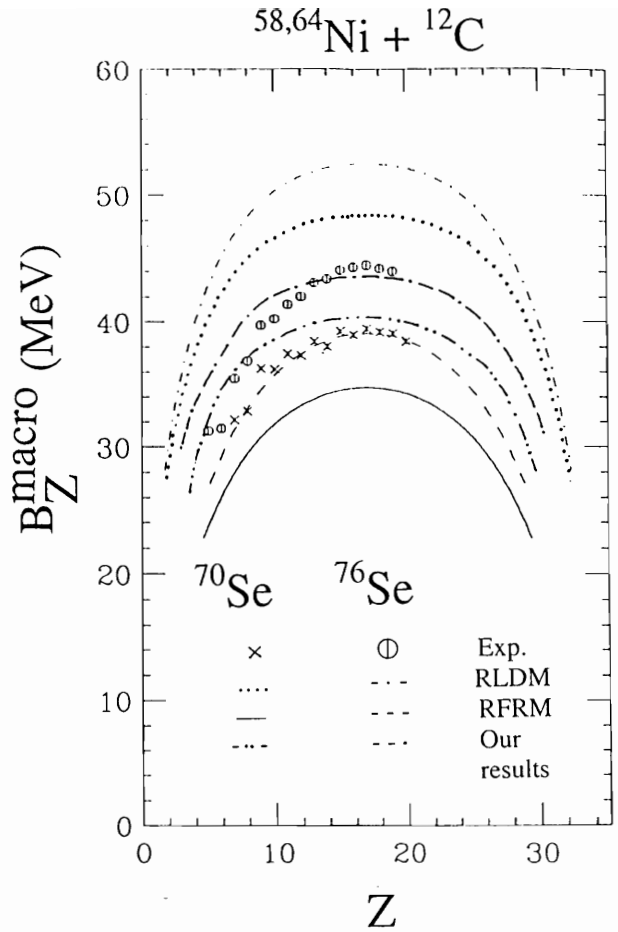

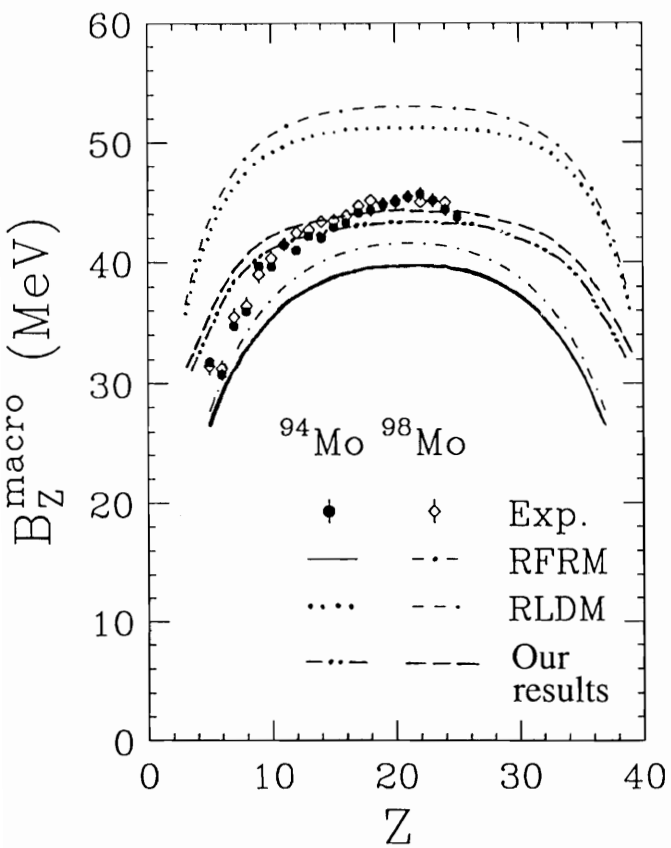

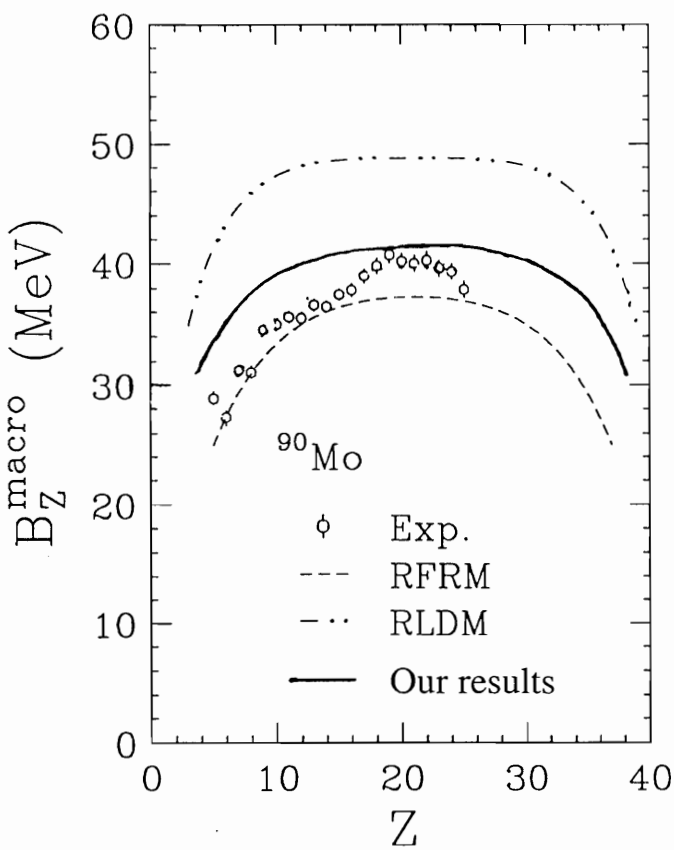

Figures1,2 and 3. Experimental asymmetric fission barrier heights corrected for shell effects are compared to Rotating Liquid Drop Model and Rotating Finite Range Model predictions and to our results for ^{70,76}Se, ^{94,98}Mo and ^{90}Mo.

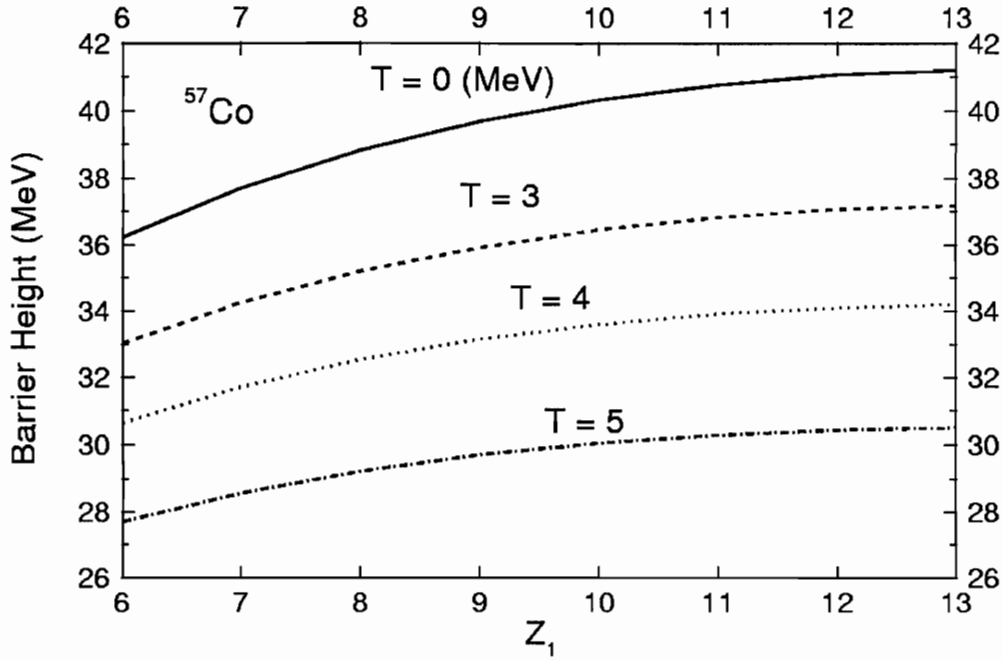

Figure 4. Fission barrier heights as functions of the charge of one fragment and the temperature for the light nucleus ^{57}Co.

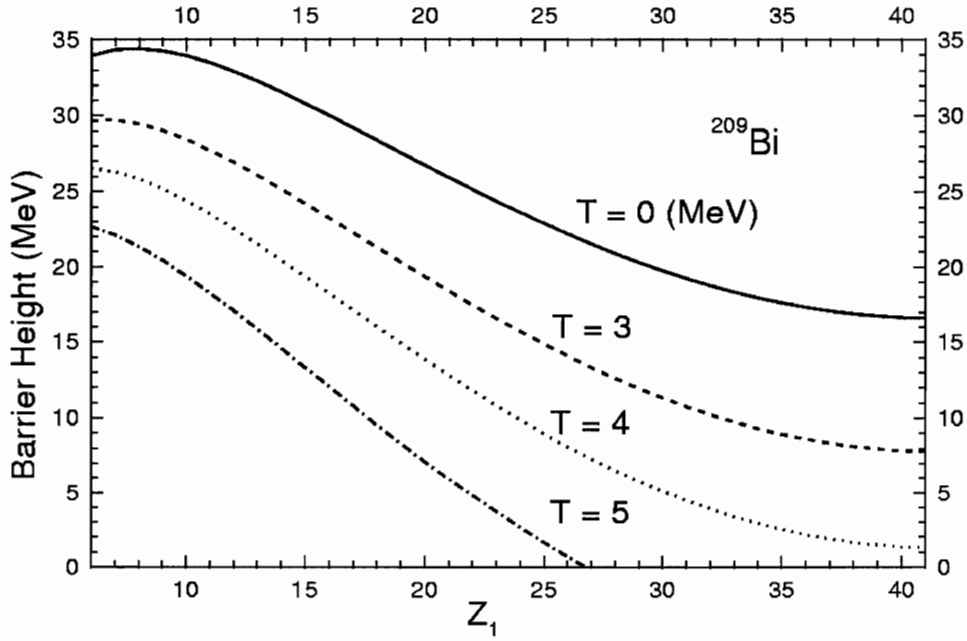

Figure 5. Fission barrier heights as functions of the charge of one fragment and the temperature for the heavy nucleus ^{209}Bi.

Z	A	(Z_1, A_1, E_{bar} (MeV))									
30	62	(5, 9, 33.1)	(7, 13, 36.7)	(8, 15, 37.8)	(9, 18, 38.7)	(10, 20, 39.4)	(11, 22, 39.9)	(12, 24, 40.2)	(13, 26.5, 40.5)	(14, 29, 40.6)	(15, 31, 40.7)
	65	(5, 10, 35.3)	(7, 15, 38.6)	(8, 17, 39.8)	(9, 19, 40.7)	(10, 21, 41.4)	(11, 24, 41.9)	(12, 26, 42.3)	(13, 28, 42.6)	(14, 30, 42.7)	(15, 32.5, 42.7)
	68	(5, 12, 37.1)	(7, 16, 40.2)	(8, 18, 41.3)	(9, 21, 42.1)	(10, 23, 42.8)	(11, 25, 43.3)	(12, 27, 43.7)	(13, 29.5, 43.9)	(14, 32, 44.1)	(15, 34, 44.1)
33	72	(5, 10, 35.3)	(7, 15, 38.7)	(8, 17, 39.8)	(9, 19, 40.7)	(10, 21, 41.4)	(11, 24, 42)	(12, 26, 42.4)	(14, 30, 43)	(15, 33, 43.1)	(16, 35, 43.2)
	75	(5, 12, 36.9)	(7, 16, 40.1)	(8, 18, 41.2)	(9, 21, 42.1)	(10, 23, 42.8)	(11, 25, 43.3)	(12, 27, 43.7)	(14, 32, 44.3)	(15, 34, 44.4)	(16, 36, 44.5)
	78	(5, 13, 38.7)	(7, 18, 41.5)	(8, 20, 42.4)	(9, 22, 43.2)	(10, 24, 43.8)	(11, 27, 44.2)	(12, 29, 44.6)	(14, 33, 45.1)	(15, 36, 45.2)	(16, 38, 45.2)
36	81	(5, 11, 36.2)	(7, 16, 39.5)	(8, 18, 40.6)	(9, 20, 41.5)	(10, 22, 42.2)	(12, 27, 43.2)	(14, 31, 43.8)	(15, 34, 44)	(16, 36, 44.1)	(18, 40.5, 44.2)
	84	(5, 13, 37.8)	(7, 17, 40.8)	(8, 19, 41.8)	(9, 22, 42.6)	(10, 24, 43.2)	(12, 28, 44.2)	(14, 33, 44.7)	(15, 35, 44.9)	(16, 37.5, 45)	(18, 42, 45.1)
	88	(5, 15, 40.3)	(7,19, 42.6)	(8, 21, 43.3)	(9, 24, 43.9)	(10, 26, 44.4)	(12, 30, 45)	(14, 35, 45.4)	(15, 37, 45.5)	(16, 39.5, 45.5)	(18, 44, 45.6)
39	86	(5, 10, 35.4)	(6, 12, 37.2)	(7, 14, 38.5)	(8, 17, 39.6)	(10, 21, 41.1)	(12, 26, 42)	(14, 30, 42.6)	(16, 35, 42.9)	(18, 40, 43)	(19, 42, 43.1)
	89	(5, 11, 36.4)	(6, 14, 38.2)	(7, 16, 39.5)	(8, 18, 40.6)	(10, 23, 42.1)	(12, 27, 43.1)	(14, 32, 43.7)	(16, 36.5, 44.1)	(18, 41, 44.2)	(19, 43, 44.3)
	92	(5, 13, 37.9)	(6, 15, 39.5)	(7, 17, 40.8)	(8, 20, 41.8)	(10, 24, 43.1)	(12, 29, 44)	(14, 33, 44.5)	(16, 38, 44.8)	(18, 43, 45)	(19, 45, 45)
42	92	(5, 9, 35.3)	(6, 11, 37.1)	(7, 14, 38.4)	(8,16, 39.3)	(9, 18, 40)	(11, 23, 40.9)	(13, 27.5, 41.5)	(15, 32, 41.8)	(17, 37, 41.9)	(21, 46, 42)
	96	(5, 11, 36.1)	(6, 13, 37.9)	(7, 16, 39.2)	(8, 18, 40.2)	(9, 20, 41)	(11, 25, 42.2)	(13, 29.5, 42.9)	(15, 34, 43.3)	(17, 39, 43.5)	(21, 48, 43.7)
	100	(5, 13, 37.9)	(6, 15, 39.5)	(7, 18, 40.7)	(8, 20, 41.6)	(9, 22, 42.3)	(11, 27, 43.3)	(13, 31.5, 43.9)	(15, 36, 44.3)	(17, 41, 44.5)	(21, 50, 44.6)
45	101	(5, 10, 35.7)	(6, 12, 37.3)	(7, 14.5, 38.6)	(8, 17, 39.5)	(9, 19, 40.2)	(11, 24, 41.1)	(13, 28, 41.6)	(15, 33, 41.9)	(17, 38, 42)	(22, 49, 42.1)
	103	(5, 11, 35.9)	(6, 13, 37.6)	(7, 15.5, 38.8)	(8, 18, 39.8)	(9, 20, 40.5)	(11, 25, 41.6)	(13, 29, 42.2)	(15, 34, 42.5)	(17, 39, 42.7)	(22, 50, 42.8)
	106	(5, 12, 36.8)	(6, 15, 38.4)	(7, 17, 39.7)	(8, 19, 40.6)	(9, 22, 41.4)	(11, 26, 42.4)	(13, 31, 42.9)	(15, 35.5, 43.3)	(17, 40, 43.5)	(22, 52, 43.6)
48	109	(5, 10, 35.8)	(6,12, 37.4)	(7, 15, 38.5)	(8, 17, 39.4)	(9, 19, 40)	(10, 22, 40.7)	(12, 26, 41.1)	(16, 36, 41.4)	(20, 45, 41.4)	(24, 54.5, 41.4)
	112	(5, 11.5, 36)	(6, 14, 37.6)	(7, 16, 38.8)	(8, 18.5, 39.8)	(9, 21, 40.5)	(10, 23, 41)	(12, 28, 41.7)	(16, 37, 42.2)	(20, 47, 42.2)	(24, 56, 42.2)
	115	(5, 13, 37.1)	(6, 15, 38.6)	(7, 18, 39.7)	(8, 20, 40.6)	(9, 22, 41.3)	(10, 25, 41.8)	(12, 29, 42.4)	(16, 39, 42.8)	(20, 48, 42.8)	(24, 57.5, 42.8)
51	121	(5, 12, 36.1)	(6, 14.5, 37.6)	(7, 17, 38.8)	(8, 19, 39.6)	(10, 24, 40.7)	(12, 29, 41.3)	(14, 33, 41.5)	(16, 38, 41.6)	(21, 50, 41.4)	(25, 59, 41.3)
	123	(5, 13, 36.9)	(6, 15.5, 38.3)	(7, 18, 39.4)	(8, 20, 40.2)	(10, 25, 41.2)	(12, 30, 41.7)	(14, 34, 41.9)	(16, 39, 41.9)	(21, 51, 41.7)	(25, 60, 41.6)
	126	(5, 15, 38.6)	(6, 17, 39.9)	(7, 19, 40.8)	(8, 22, 41.4)	(10, 26, 42.1)	(12, 31, 42.4)	(14, 36, 42.5)	(16, 40.5, 42.4)	(21, 52, 42.1)	(25, 62, 41.9)
54	126	(5, 11, 35.7)	(6, 13, 37.1)	(7, 15, 38.2)	(8, 18, 38.9)	(10, 22.5, 39.8)	(13, 30, 40.2)	(15, 34, 40.2)	(20, 46, 39.7)	(24, 56, 39.4)	(27, 63, 39.3)
	131	(5, 13, 36.5)	(6, 16, 37.9)	(7, 18, 39)	(8, 20, 39.7)	(10, 25, 40.6)	(13, 32, 41)	(15, 37, 41)	(20, 48, 40.6)	(24, 58, 40.3)	(27, 65.5, 40.2)
	136	(5, 16, 39.8)	(6, 18, 40.8)	(7, 20, 41.5)	(8, 23, 41.9)	(10, 27.5, 42.2)	(13, 35, 42.1)	(15, 39, 41.2)	(20, 51, 40.9)	(24, 61, 40.6)	(27, 68, 40.5)
57	136	(5, 12, 35.5)	(6, 14, 36.9)	(7, 16.5, 37.9)	(8, 19, 38.6)	(10, 24, 39.4)	(13, 31, 39.7)	(18, 43, 39.2)	(20, 48, 38.9)	(24, 57, 38.3)	(28, 67, 38.1)
	139	(5, 13, 36.2)	(6, 16, 37.5)	(7, 18, 38.5)	(8, 20, 39.2)	(10, 25, 39.9)	(13, 32, 40.2)	(18, 44, 39.6)	(20, 49, 39.3)	(24, 59, 38.8)	(28, 68, 38.5)
	142	(5, 15, 37.8)	(6, 17, 39)	(7, 19.5, 39.8)	(8, 22,40.3)	(10, 27, 40.8)	(13, 34, 40.8)	(18, 46, 40)	(20, 51, 39.6)	(24, 60, 39)	(28, 70, 38.8)
60	142	(5, 11, 35.6)	(6, 13, 36.8)	(7, 15.5, 37.7)	(9, 20, 38.7)	(11, 25, 38.9)	(13, 30, 38.8)	(17, 39.5, 38)	(21, 49, 37)	(24, 56.5, 36.4)	(30, 71, 35.9)
	144	(5, 12, 35.3)	(6, 14, 36.6)	(7,16.5, 37.5)	(9, 21, 38.6)	(12, 28.5, 39)	(14, 33, 38.8)	(17, 40.5, 38.2)	(21, 50, 37.3)	(24, 57.5, 36.8)	(30, 72, 36.3)
	148	(5, 14, 36.2)	(6, 16, 37.4)	(7, 18.5, 38.3)	(9, 23, 39.2)	(12, 30.5, 39.5)	(14, 35, 39.3)	(17, 42.5, 38.7)	(21, 52, 37.8)	(24, 59.5, 37.3)	(30, 74, 36.8)

Table 1. Asymmetric fission barrier heights (T=0) in the deformation path through compact quasi-molecular configurations. The height (in MeV) is given by the third number in parenthesis as functions of the charge and mass Z and A of the fissioning nucleus and the charge Z_1 of the detected fragment of most probable mass A_1.